Solid State Ionics 276 (2015) 136–141

Contents lists available at ScienceDirect

Solid State Ionics

journal homepage: www.elsevier.com/locate/ssi

Temperature and pressure dependence of electrical conductivity in synthetic anorthite

Haiying Hu [a,b], Lidong Dai [a], Heping Li [a,*], Keshi Hui [a,c], Jia Li [a,c]

[a] Key Laboratory for High-temperature and High-pressure Study of the Earth's Interior, Institute of Geochemistry, Chinese Academy of Sciences, Guiyang, Guizhou 550002, China
[b] Key Laboratory of Earth and Planetary Physics, Institute of Geology and Geophysics, Chinese Academy of Sciences, Beijing 100029, China
[c] University of Chinese Academy of Sciences, Beijing 100039, China

ARTICLE INFO

Article history:
Received 29 December 2014
Received in revised form 14 April 2015
Accepted 15 April 2015
Available online 1 May 2015

Keywords:
Anorthite
Electrical conductivity
Transport mechanism
Diffusivity

ABSTRACT

Electrical conductivity measurements of synthetic anorthite were carried out as a function of pressure and temperature by a Solartron-1260 Impedance/Gain phase analyzer in a multi-anvil apparatus. The impedance spectroscopy was performed in a frequency range from 10–1 Hz to 106 Hz. The sample was synthesized at 1673 K in a high temperature furnace. Our experimental results show that (1) a dramatic increase in electrical conductivity with increasing temperature and a slightly decrease in conductivity with increasing pressure at constant temperature, however, the effect of pressure on the conductivity is less pronounced than that of temperature; (2) the activation enthalpy linearly increases with increasing pressure (1.86–1.91 eV) reflecting the mobility of $Ca2^{+}$ decreases as the anorthite framework becomes more compressed; (3) the activation energy at atmospheric pressure and activation volume are 1.83 eV and 2.39 cm^3/mol, respectively; (4) According to these Arrhenius parameters, it is proposed that the possible dominant mechanism of the charge transport in anorthite under experimental conditions is the hopping of $Ca2^{+}$ from one near aluminum oxygen site to another; (4) the diffusion coefficient of calcium was calculated from the present conductivity data using Nernst–Einstein equation, and compared with previous experimental results.

1. Introduction

Feldspars are the most abundant rock-forming minerals and constitute 60% of the Earth's crust, and are widely present in variety of igneous and metamorphic rocks [1]. Anorthite, as one of end-numbers in feldspars, has a large stability field, which extend to 3 GPa in pressure and to below 1000 °C in temperature [2–4]. Consequently, anorthite would play an important role in the composition of the uppermost upper mantle when it effectively plunge the continental slab into the mantle.

Electrical conductivity is one of the significant parameters to place constraints on the thermal structure and composition of the Earth's interior since it is highly sensitive to thermodynamic parameter such as temperature, pressure and chemistry of the constituent materials [5–7]. Laboratory-based electrical conductivity of geomaterials can provide independent data to help the interpretation of the field magnetotelluric results and borehole data. The electrical conductivity of anorthite would therefore make a significant contribution to the electrical structure of the Earth's crust and the uppermost upper mantle. In addition, the study on conduction behavior of anorthite at high temperature and pressure can aid in understanding the charge transport mechanism, and is an efficient probe of mass transfer processes for the diffusion. The electrical properties of feldspars have been the subject of numerous studies for decades [8–22], however, most previous studies are extensively concerning in the electrical conductivities of alkali feldspar and plagioclase with intermediate composition. Extremely limited publications reported the electrical conductivity of end-number anorthite. Maury [11] studied the electrical conductivity of the whole feldspar family, both natural and synthetic, at 672–1173 K and ambient pressure using impedance spectroscopy method, and the results indicated that the activation energies for all feldspars vary in the range of 0.72–0.87 eV. Recently, Bagdassarov et al. [15] investigated the variation of activation energy of electrical conductivity with pressure in order to determine the pressure dependence of anorthite glass transition, however, their aim was to discriminate glassy and liquid states by measuring the electrical conductivity of anorthite glass at high temperature, not focus on anorthite crystal over its stability field. Notably, no study has yet reported the electrical conductivity of anorthite crystal simultaneously under high temperature and high pressure condition.

As one of our systematic study on electrical property of feldspar family which have been partly reported in Hu et al. [19–21], the electrical conductivity of synthetic anorthite is measured at 1.0–3.0 GPa and 873–1173 K by means of complex impedance spectroscopy in a multi-anvil high-pressure apparatus. We discuss the conduction mechanism of anorthite at high temperature in details using the experimental results, and the diffusion coefficient of calcium was calculated from

* Corresponding author.
E-mail address: hepingli_2014@hotmail.com (H. Li).

http://dx.doi.org/10.1016/j.ssi.2015.04.008
0167-2738/

the conductivity data by using Nernst–Einstein equation, and compared it with previous Ca tracer diffusion coefficient.

2. Experimental procedures

2.1. Sample preparation

High-pure silicon dioxide (SiO2), aluminum oxide (Al2O3) and calcium carbonate (CaCO3) was used to prepare the starting material. The preparation of the experimental sample is carried out by the following two steps. (1) The oxide powders firstly were weighed, then mixed and ground under acetone in an agate mortar for 2 h. In order to remove the possible water, the mixtures were dried at 723 K for 4 h. The anorthite subsequently was synthesized in a stepwise fashion, and then kept at 1673 K under ambient pressure for 3 h in high temperature furnace and finally slowly cooled down to room temperature. The experimental products were confirmed to be anorthite crystals by the micro-focused X-ray diffractometer. (2) In order to obtain the cylindrical sample, the synthetic anorthite powder were ground again under ethanol in an agate mortar and dried at 723 K in a muffle furnace, then loaded into a copper capsule. The sample eventually was sintered at 573 K and 2.0 GPa for 1 h in multi-anvil apparatus in order to reduce porosity in the sample. The sintered sample was then cut and polished into the cylinder with a diameter of 6.0 mm and a height of 6.0 mm for subsequent electrical conductivity measurement. Finally, the sample was cleaned successively in acetone and ethanol using an ultrasonic cleaner, and later keeping dry in an oven before the sample assembly. The texture of the sample was examined using scanning microscope (SEM), which showed the foam texture and the grain size was nearly uniform (Fig. 1). The chemical composition was determined by EPMA-1600 electron probe (EMPA) operated at 25 kV and 10 nA and the results were showed in Table 1.

2.2. Electrical conductivity measurements

Electrical conductivity measurements were carried out in an YJ-3000t multi-anvil apparatus. The sample assembly for the conductivity measurement resembles that in our previous studies [19–21]. The aluminum oxide (Al2O3) insulator, hexagonal boron nitride (HBN) sleeve, cubic pyrophyllite pressure media and other parts were heated at 1023 K for 5 h in a muffle furnace prior to sample assembly. The cylindrical sample was placed in a HBN sleeve with an inner diameter of 6.0 mm, and sandwiched by two Pt electrodes with the same diameter as HBN. After completing the assembly, it was further dried at 473 K in an oven overnight before the electrical conductivity measurement. In order to check the distortion of sample geometry during conductivity measurement, the sample cell after measurement was polished to section and the cross-section was shown in Fig. 2 in which the original sample geometry was largely preserved. Therefore, the distortion of sample dimension can be neglected during data processing.

Table 1
The chemical composition of synthetic anorthite by electron microprobe analysis (wt.%).

Oxide	Synthetic anorthite
SiO2	43.41
Al2O3	35.33
CaO	20.83
Cr2O3	0.04
Na2O	0.15
total	99.76

Impedance spectroscopy measurements were carried out in a multi-anvil apparatus by a Solartron 1260 impedance gain-phase analyzer at 873–1173 K and 1.0–3.0 GPa, with the applied alternating current voltage of 1 V in the frequency range of 10^{-1}–10^{6} Hz. Since water has a significant effect on the conductivity measurement, two or three heating and cooling cycles were undertaken to drive off any moisture in cell assembly and sample. For each run, the sample was firstly compressed to the desired pressure with a rate of 1.5 GPa/h. Then the temperature was changed in 50 K steps and simultaneously the impedance spectra were collected in subsequent heating or cooling cycles. The experimental results showed that the conductivity data from the first heating cycle obviously deviated from other cycles, therefore, only the reproducible data were chosen for the analysis process.

Impedance spectra showed that one semicircular arc and one small tail in the high and low frequency range, respectively. As the tail following the arc corresponds to grain boundary transport or sample-electrode interface process (discuss below), the semicircular arc representing the bulk conduction property is fitted by using an equivalent circuit of resistor and capacitor in parallel to obtain sample resistance. The conductivity was then calculated from the sample resistance and dimensions using the equation, $\sigma = L/SR$, where σ is the electrical conductivity, L and S are the sample length and cross-section area of electrode, respectively, and R is the sample resistance. Experimental errors are mainly from (1) the fitting error of impedance arcs that are no more than 5%, and (2) the uncertainty of temperature which is less than 10 K due to the thermal gradient along the length of sample cell. The error arising from the distortion of sample dimension can be neglected since the sample after conductivity measurement reserved its original geometry as shown in Fig. 2. Therefore, the total uncertainty of electrical conductivity is not more than 5%.

3. Results

Fig. 3 shows the typical impedance spectra of sample at 1.0 GPa. Each impedance spectrum shows one semicircular arc at high frequencies

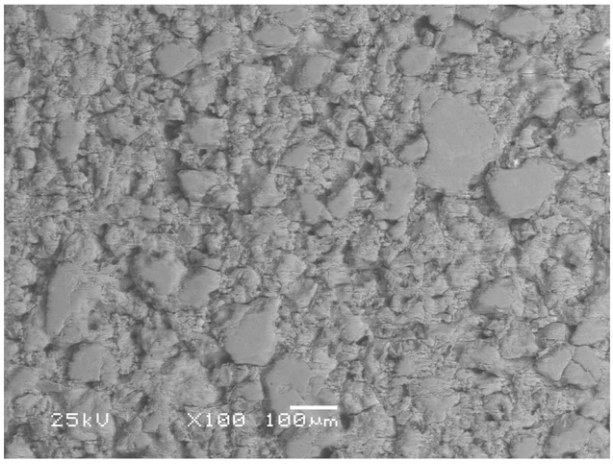

Fig. 1. Cross-section of the recovered sample cell from an electrical conductivity measurement. The original sample geometry was largely preserved.

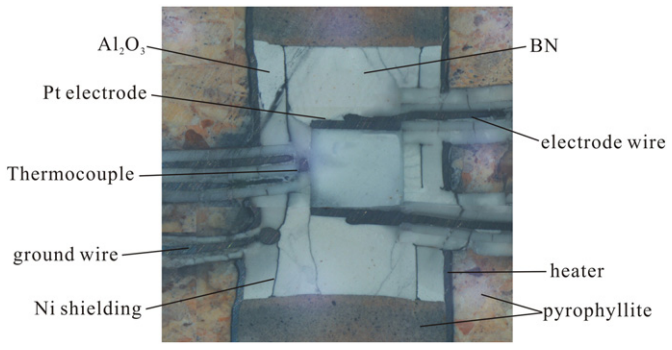

Fig. 2. Backscattered electron image of the microstructure of the sample after the conductivity measurements.

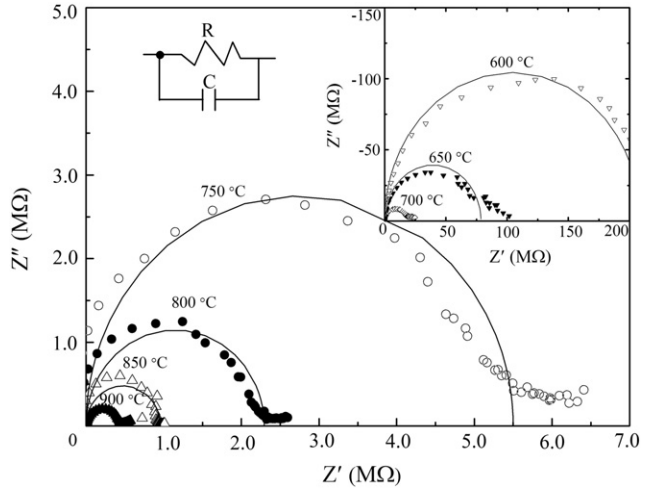

Fig. 3. Complex impedance spectra of anorthite from 0.1 to 106 Hz at 1.0 GPa and 873–1173 K. Z′ and Z″ are the real and imaginary part of complex impedance, respectively. An equivalent circuit of a single resistor (R) and capacitor (C) in parallel was used to fit the impedance arc in the high frequency region. The solid semi-circular lines are the fitting results of impedance arcs.

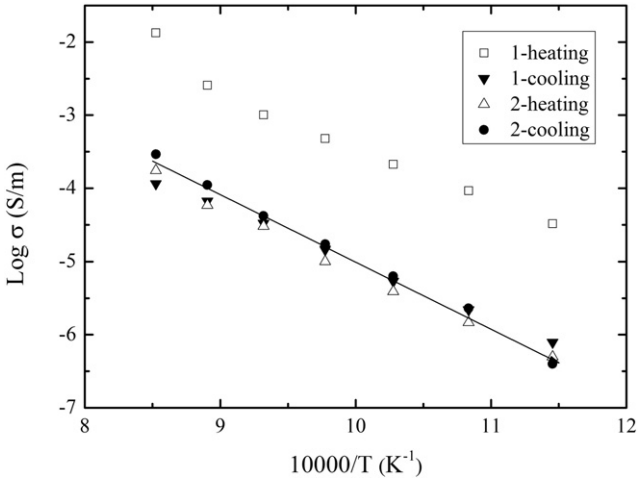

Fig. 4. The logarithm of electrical conductivity versus reciprocal temperature for anorthite in different heating/cooling cycles at 1.0 GPa. Data from the first heating cycle were precluded during the analysis process.

and an additional part appearing at lower frequencies. The semi-circular arc of a center that falls on the real axis corresponds to the grain interior conduction process. The tail following the arc in complex impedance plane is usually attributable to grain boundary transport or sample-electrode process. Generally, the complete arc representing grain boundary conduction occurs at the intermediate frequency range of 0.01–200 Hz, and has a different characteristic relaxation time [23, 24], whereas the grain boundary arc was not observed after the grain interior arc as shown in Fig. 3. Accordingly, the electrode response can appear as a separate or as a straight line which is a characteristic of diffusion process at the sample-electrode interface [25, 26], so the low frequency tail in this study reflects an effect of the electrodes. Therefore, the bulk sample resistance was determined from the first arc by modeling the electrical response with an equivalent circuit of resistor and capacitor in parallel as shown in Fig. 3.

Since the linear relation of the logarithmic conductivity against the reciprocal temperature, the electrical conductivity can be expressed by Arrhenius's formula:

$$\sigma = A\exp\left(-\frac{\Delta H}{kT}\right) \tag{1}$$

where A is a pre-exponential factor (S/m), k is the Boltzmann constant (eV/K), T is the absolute temperature (K) and ΔH is the activation enthalpy (eV), the pressure dependency of which could be expressed by $\Delta H = \Delta E_0 + P\Delta V$, where ΔE_0, ΔV and P are correspondent to the activation energy at atmospheric pressure, activation volume and pressure, respectively. The electrical conductivity from different cycles at 1.0 GPa and the reproducible data at 1.0–3.0 GPa are illustrated in Figs. 4 and 5, respectively. Accordingly, the parameters from fitting Eq. (1) to the data are shown in Table 2, in which the activation energy and activation volume are 1.83 eV and 2.39 cm^3/mol, respectively.

As shown in Fig. 4, the conductivity data from first heating cycle are apparently higher than these from subsequent heating and cooling cycles. The moisture in cell assembly or the absorbed water in sample probably gives rise to the deviation of electrical conductivity, which is also observed in previous studies [18]. On the basis of the reproducibility from the second cycle in Fig. 4 and the high activation enthalpy (>1.80 eV) shown in Table 2, it is implied that water doesn't play a significant role on electrical conductivity in this study. Therefore, in order to obtain the reproducible data, the same heating/cooling cycle measurements are performed at 2.0 GPa and 3.0 GPa and the data from the first heating cycle are excluded during data analysis process.

As shown in Fig. 5, the electrical conductivity increase by about 2.5 order of magnitude with increasing temperature from 673 to 1173 K at constant pressure. Conversely, the electrical conductivity decreases by nearly 0.5 log unit from 1.0 GPa to 3.0 GPa at a constant temperature, and accordingly the activation enthalpy slightly increases from 1.86 eV to 1.91 eV as shown in Table 2, which indicate that the ionic mobility decreases as the anorthite framework becomes more compressed. Accordingly, the lattice parameters decrease and the internal energy increases with pressure. As a result, the pathways of carriers could become narrower and more energy is required for carriers across the energy barrier, which ultimately reflects the reduction of electrical conductivity and the rise of activation enthalpy. The amount of increase in activation enthalpy is reflected by the sum of pressure and activation volume (2.39 cm^3/mol) obtained in our present studies.

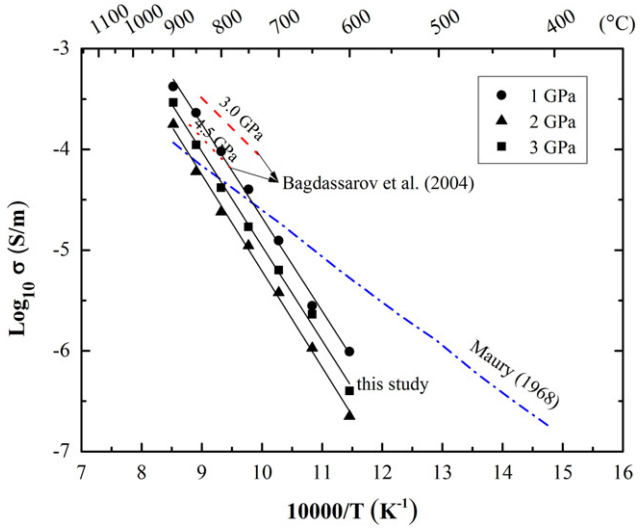

Fig. 5. Electrical conductivity of anorthite as a function of reciprocal temperature at 1.0–3.0 GPa. The solid lines indicate the fitting results from this study. The red dashed line and the dotted line denote the conductivity data of anorthite glass at 3.0 GPa and 4.5 GPa, respectively [15]. The blue dot-dashed line shows the previous result for synthetic anorthite at ambient pressure from Maury [11].

Table 2
Fitting parameters for electrical conductivity of synthetic anorthite in present study together with previous results. An, anorthite.

Run no.	P (GPa)	T (K)	Log A	A (S/m)	ΔH (eV)	ΔE0 (eV)	ΔV (cm^3/mol)	References
A103	1.0	873–1173	4.62±0.26	41687	1.86±0.03	1.83±0.01		This study
A113	2.0	873–1173	4.43±0.23	26915	1.88±0.02		2.39±0.28	
A127	3.0	873–1173	4.36±0.23	18621	1.91±0.04			
Synthetic An	10–4	673–1173	−0.20		–	0.87	–	Maury [11]
Anorthite	3.0	1000–1250	–	–	–	1.22	–	Bagdassarov et al. [15]
	4.5					1.50		

4. Discussion

4.1. Comparison with previous results

Since the electrical conductivity data on anorthite are very scarce, only two sets of similar data are chosen to compare with our results as shown in Fig. 5. Maury [11] performed the systematic measurements on the electrical conductivity feldspar including synthetic anorthite at 673–1173 K and ambient pressure. Their data indicated that at lower temperature (<750 K) the electrical conductivities are apparently higher than our results, but in a higher temperature region (>750 K) they are slightly lower. This is attributed to the smaller temperature dependence (activation energy) of electrical conductivity compared to ours. These differences can be explained by the difference in the experimental pressures. In this study the electrical conductivity was measured at pressures of 1.0–3.0 GPa, whereas Maury [11] performed the conductivity measurement at ambient pressure. According to the effect of pressure on the electrical conductivity in this study, it is reasonable that our results are lower than that of Maury's [11]. The discrepancy of the activation energy between these two studies can be attributed to the different sample synthetic methods, since the variation in activation energy for samples with the same composition may depend on the different preparation methods [6]. Owing to the absence of information about sample synthetic process by Maury [11], it is difficult to distinguish the exact difference in sample synthetic method between these two studies.

Bagdassarov et al. [15] reported the glass transition temperature from the pressure effect on the activation energy of electrical conductivity in alkali, alkaline earth (anorthite) silicate and SiO2 glasses using AC impedance spectroscopy method. The electrical conductivity of anorthite before phase transition at 3.0 and 4.5 GPa was chosen to compare with our results as shown in Fig. 5. Noticeably, at 3.0 GPa their conductivity data are by more than 0.5 order of magnitude higher than the present results at the same pressure, and the activation enthalpies (e.g., 1.17 eV at 3.0 GPa and 1.22 eV at 4.5 GPa) are much lower than our result (1.91 eV). However, the decrease of electrical conductivity and the increase of activation enthalpy with increasing pressure from their data resemble in this study. The discrepancy in electrical conductivity and activation energy can be explained by the difference of respective sample. The sample used by Bagdassarov et al. [15] is anorthite glass which is quite different from our crystalline sample used by us. Generally, many of physical properties including electrical conductivity are intimately related to the structure of material, depending on the working temperature [27]. For the silicate glass, the silicon–oxygen tetrahedra (SiO4) are connected irregularly and form a disordered three-dimensional network. Alkali and alkaline–earth elements as the network modifiers are filling the holes in this random network, and bonded with non-bridging oxygens (NBOs) and participating in network depolymerization [28, 29]. In the case of anorthite glass, calcium can play different structural roles either as modifiers, participating in network depolymerization and bonded with non-bridging oxygens, or as charge compensators, near the (AlO4)− tetrahedra and bonded with bridging oxygens, ultimately, perturbing the polymerized network [28]. Accordingly, the less stronger linkage of Ca ions to the glass network would cause that the free energy required to move the defect across the energy barrier in glass may be smaller compared to crystalline due to the lower degree of polymerization, which implies that the higher electrical conductivity and the lower activation enthalpy as investigated by Bagdassarov et al. [15].

4.2. Conduction mechanism

The electrical conductivity of a material is the sum of the conduction of each charge carrier (or defect) type acting in parallel

$$\sigma = \sum N_i q_i \mu_i \tag{2}$$

where N_i is the density of the i-th type of charge carrier, q_i is its effective charge ($q_i = z_i e_i$), and μ_i is its mobility. Owing to the dependence of the activation energies for each conduction mechanism on those of the charge mobility, all conduction mechanisms can be distinguished by different slop (activation energy) defined in a specific temperature region on the Arrhenius plot. In the case of synthetic anorthite in the present study the Arrhenius plot showed that there is only a linear relation between electrical conductivity and temperature, which implied that only one conduction mechanism can be identified.

Generally, conduction by diffusion of ions is characterized by a high activation energy (>2 eV) and a positive activation volume (i.e., conductivity decreases with increasing pressure) due to the difficulty for formation and migration of cation vacancies at high pressures [30]. The present study demonstrated that the activation enthalpy is nearly 2.0 eV and the activation volume is a positive value (2.39 cm^3/mol), therefore, the hopping of ions in lattice can be made a significant contribution to the electrical conductivity of anorthite under our experimental condition. In anorthite crystal structure, calcium ions are proposed to be the dominant charge carriers due to their relatively higher mobility in comparison with other component elements such as oxygen, silica and alumina ions, which comprise an aluminosilicate framework of corner sharing Si- and Al-tetrahedra. According to the previous diffusion studies, the activation energy for oxygen diffusion in anorthite (An97) under anhydrous condition is 2.45 eV at ambient pressure and in the temperature region of 850–1300 °C [31], and the activation energy for Si diffusion in anorthitic feldspar (An93) was 4.82 eV under dry and low pressure condition [32]. Although the aluminum diffusion data in anorthite is scarce, one could expect for aluminum diffusion an activation enthalpy of nearly that of Si diffusion due to the substitution of an Al^{3+} for a Si^{4+} in a tetrahedron. Consequently, we suggest that calcium ions in anorthite make the dominant contribution to the electrical conduction at high temperature and high pressure, as pointed out by Bagdassarov et al. [15] for the anorthite glass although the activation energy (~1.20 eV) they obtained is much lower than ours (~1.90 eV).

Other conduction mechanisms, such as proton and small polaron conduction which is the hopping of electron holes between ferrous and ferric iron, are not likely to make an important role in conduction for anorthite. Proton conduction is considered to be an important conduction mechanism when nominally anhydrous minerals contain a certain amount of structural water. Because the proton is an extremely small ion, the activation enthalpy for such a fast migration process of extrinsic impurities is expected to be much lower than that for ion. The experimentally determined activation enthalpy is around 0.9 eV, which is extensively reported in silicate minerals such as hydrous

olivine and its high-pressure polymorphs [33–37], orthopyroxene [38, 39], garnet [40] and enstatite [39]. For small proton conduction, it is proposed as a main conduction mechanism in the main iron-bearing minerals, e.g., olivine, garnet, ferro-periclase, silicate perovskites [41–51]. These studies have been shown that small polaron conduction is characterized by a negative activation volume and a relative low activation energy (1~1.5 eV). Thus, the positive activation volume (2.39 cm^3/mol), the higher activation energy (~1.90 eV) and the iron-free sample in this study rule out any significant contribution of proton and small polaron to the conduction. Calcium ions are the best candidates acting as charge carriers in anorthite, and hop in lattice along the applied electric field direction.

4.3. Calculation of the Ca diffusion coefficient

Basically the electrical conductivity is the diffusion of charge-carrying species. For our anorthite sample, only calcium ions are suggested to make a significant contribution to the bulk conductivity, thus its diffusion coefficient can be calculated through Nernst–Einstein equation [52]:

$$D = H_r \sigma kT / nq^2 \quad (3)$$

where D is the diffusion coefficient, Hr is the Haven ratio related to the correlation factor, k and T are the Boltzmann constant and absolute temperature, respectively, q is the charge, n is the number of charge carrier per volume unit expressed as $n = N_A \rho L/M$, where NA is the Avogadro's number, ρ is the density of anorthite, M is the molecular weight, and L is the number of calcium atoms in a molecule. The Haven ration Hr generally has a value in the range of 0.1 to 1.0 depending on the nature of diffusion mechanism. For the interstitial mechanism, the Haven ratio usually equals to 1.0, but for the vacancy or interstitially mechanism, it is less than 1.0 [53]. According to previous diffusion experiments on alkali feldspar, Na^+ diffusion is primarily by an interstitial mechanism due to the smaller ionic radius, whereas K^+ and alkali cations with large ionic size are proposed to move mainly by vacancy mechanisms or others [54,55]. Although the Ca self-diffusion coefficient in natural anorthite was reported by LaTourrette and Wasserburg [56], the Ca diffusion mechanism has not yet been discussed in detail. One would expect that the Ca diffusion is by a vacancy mechanism or other strongly correlated movement owing to the much larger ionic radius compared to that of Na^+ and K^+. Because the accurate Haven ratio is unavailable for anorthite, $Hr = 0.1$ was assumed in order to simplify the calculation. Using Eq. (3) and assuming only Ca ions are involved in the transport process, we calculated its diffusion coefficient from the conductivity data of synthetic anorthite under the present experimental conditions, and the results are illustrated in Fig. 6 together with the diffusion coefficient measured by way of Fick's law.

As demonstrated in Fig. 6, the calculated Ca diffusion coefficients fall in a range of 10–19–10–15 m^2/s at temperatures of 873–1173 K and high pressure. Comparison with previous diffusion results is very difficult because experimental diffusion data of pure anorthite unfortunately have heretofore been unavailable at temperature below 1000 °C. The diffusion data at high temperature are also very limited, and only two sets of data for plagioclase are available to compare with our calculated results as indicated in Fig. 6. LaTourrette and Wasserburg [56] performed the measurement on the self-diffusion coefficients of Ca in natural anorthite (An95) parallel to both b and c-direction at 1200–1400 °C and ambient pressure using a diffusion couple method. Behrens et al. [57] measured the Ca diffusion coefficient in plagioclase (An60) at 1 bar and 1000–1300 °C by residual activity method using the radioactive isotope ^{45}Ca. Obviously, the calculated results in this study are much higher than both of those from LaTourrette and Wasserburg [56] and Behrens et al. [57] if both of their data are extrapolated to lower temperature (<1000 °C). By contrast, the slopes of the Arrhenius plots (the activation energy) in the present study are markedly smaller than these previous experimental results: this study, 1.83 eV; LaTourrette and Wasserburg [56]: ~2.60 eV; and Behrens et al. [57]: 3.25 eV. These discrepancies in diffusion coefficient and activation energy can be attributed to the difference in the experimental method, temperature, pressure and samples in respective measurement. The experimental method used by us is completely different from these of LaTourrette and Wasserburg [56] and Behrens et al. [57]. The calculated Ca diffusion coefficient in the present study is the basis on many assumptions, for instance, the value of HR, only Ca ions contribution to conductivity, thus it does not correspond to the diffusion coefficient directly measured by way of Fick's law. However, we note that the calculated diffusion coefficient has the dimensions of a tracer diffusion coefficient, therefore, our results can provide a significant independent constraint on the experimentally determined values. Calcium is a major constituent element of plagioclase, the diffusion of which is important in understanding high-temperature processes such as metamorphic reactions, exsolution kinetics, creep, and phase transformation [32, 58], therefore, more studies on Ca diffusion measurements performed under low temperature and high pressure are required.

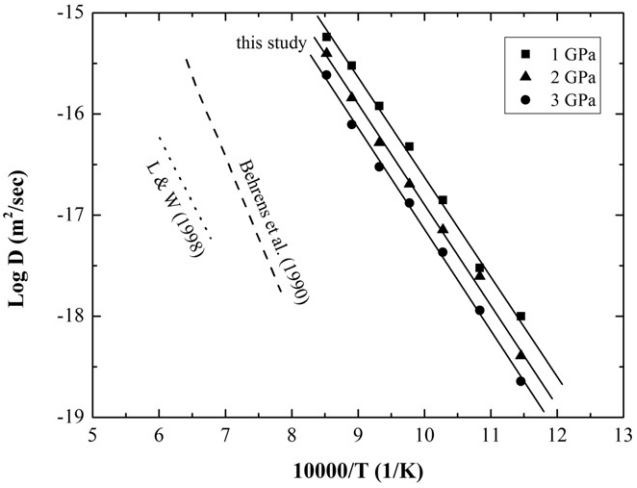

Fig. 6. The calculated $Ca2^+$ diffusion coefficient in synthetic anorthite inferred from electrical conductivity data using the Nernst–Einstein relation under experimental conditions. The dotted line illustrates that the self-diffusion coefficients of Ca in natural anorthite (An95) at atmospheric pressure and 1200–1400 °C from LaTourrette and Wasserburg [56]. The dashed line represents that the experimental $45Ca2^+$ diffusivity data in plagioclase (An60) normal to (001) at 1 bar and 1000–1300 °C from Behrens et al. [57].

5. Conclusion

The electrical conductivity measurement on dry synthetic anorthite was performed at 1.0–3.0 GPa and 873–1173 K in multi-anvil apparatus using complex impedance spectroscopy. The effect of pressure and temperature on the electrical conductivity was observed, and the electrical conductivity of anorthite dramatically increases with increasing temperature, and decreases with the increase of pressure, but temperature greatly influences the electrical conductivity much more than pressure under our experimental conditions. The linear increase in activation enthalpy with increasing pressure was investigated. According to the Arrhenius parameters, e.g., the high activation energy (1.83 eV) and the positive activation volume (2.39 cm^3/mol), it is proposed that the possible dominant conduction mechanism in anorthite at high temperature is ionic conduction, and calcium ions are considered to be charge carriers hopping in lattice under electric field. On the other hand, the Ca diffusion coefficient was calculated from electrical conductivity data based on the Nernst–Einstein equation, and compared with earlier experimental data. Our calculated results can provide an independent constraint on the direct measuring results.

Acknowledgments

The authors thank Lin Chen and Jiazhuo Peng for their technical assistances in sample preparation process, and Wenqin Zheng for the use of micro-electron probe, and the two anonymous reviewers for their constructive comments and suggestions. This research was financially supported by the "135" Program of Institute of Geochemistry of CAS, Hundred talents program of CAS, Open Foundation of Institute of Geology and Geophysics of CAS, and National Natural Science Foundation of China (41304068, 41474078 and 41174079).

References

[1] P.H. Ribbe, in: I. Parson (Ed.), Feldspars and Their Reaction, Kluwer, Dordrecht, the Netherland 1994, pp. 1–49.
[2] R.J. Angel, Am. Mineral. 73 (1988) 1114–1119.
[3] L. Liu, A.E. Gorsey, Int. Geol. Rev. 49 (2007) 854–860.
[4] X. Liu, Z.Y. Hu, L.W. Deng, Acta Petrol. Sin. 26 (2010) 3641–3650.
[5] G. Nover, Surv. Geophys. 26 (2005) 593–651.
[6] A. Yoshiasa, O. Ohtaka, D. Sakamoto, D. Andrault, H. Fukui, M. Okube, Solid State Ionics 180 (6–8) (2009) 501–505.
[7] A. Pommier, Surv. Geophys. 35 (2014) 41–84.
[8] K. Noritomi, Sci. Rep. Tohoku Univ. Ser. 56 (1955) 119–126.
[9] N. Khitarov, A. Slutskiy, Geochem. Int. 2 (1965) 1034–1042.
[10] H. Mizutani, H. Kanamori, J. Phys. Earth 15 (1967) 25–31.
[11] R. Maury, Bull. Soc. Fr. Miner. Cristallogr. 91 (1968) 355–366.
[12] A.J. Piwinskii, A. Duba, Geophys. Res. Lett. 1 (1974) 209–211.
[13] A.J. Piwinskii, A. Duba, P. Ho, Can. Mineral. 15 (1977) 196–197.
[14] A.A. Guseinov, I.O. Gargatsev, Izv. Phys. Solid Earth 38 (2002) 520–523.
[15] N.S. Bagdassarov, J. Maumus, B. Poe, A.B. Slutskiv, V.K. Bulatov, Phys. Chem. Miner. 45 (2004) 197–214.
[16] V.V. Bakhterev, Dokl. Earth Sci. 420 (2008) 554–557.
[17] H. Ni, H. Keppler, M. Manthilake, T. Katsura, Contrib. Mineral. Petrol. 162 (2011) 501–513.
[18] X. Yang, H. Keppler, C. McCammon, H. Ni, Contrib. Mineral. Petrol. 163 (2012) 33–48.
[19] H. Hu, H. Li, L. Dai, S. Shan, C. Zhu, Am. Mineral. 96 (2011) 1821–1827.
[20] H. Hu, H. Li, L. Dai, S. Shan, C. Zhu, Phys. Chem. Miner. 40 (2013) 51–62.
[21] H. Hu, L. Dai, H. Li, J. Jiang, K. Hui, Mineral. Petrol. 108 (2014) 609–618.
[22] D. Wang, Y. Yu, Y. Zhou, High Press. Res. 34 (2014) 297–308.
[23] J.J. Roberts, J.A. Tyburczy, J. Geophys. Res. 96 (1991) 16205–16222.
[24] J.J. Roberts, J.A. Tyburczy, Phys. Chem. Miner. 20 (1993) 19–26.
[25] J.R. Macdonald, Ann. Biomed. Eng. 20 (1992) 289–305.
[26] J.S. Huebner, R.G. Dillenburg, Am. Mineral. 80 (1995) 46–64.
[27] L. Cormier, G. Calas, B. Beuneu, J. Non-Cryst. Solids 357 (2011) 926–931.
[28] L. Cormier, D.R. Neuville, Chem. Geol. 213 (2004) 103–113.
[29] H. Mehrer, A.W. Imre, E. Tanguep-Nijokep, J. Phys. Conf. Ser. 106 (2008) 012001.
[30] T. Yoshino, T. Katsura, Ann. Rev. Earth Planet. Sci. 41 (2013) 605–628.
[31] S.C. Elphick, C.M. Graham, P.F. Dennis, Contrib. Mineral. Petrol. 100 (1988) 490–495.
[32] D. Cherniak, Earth Planet. Sci. Lett. 214 (2003) 655–668.
[33] D. Wang, M. Mookherjee, Y.S. Xu, S. Karato, Nature 443 (2006) 977–980.
[34] C. Romano, B.T. Poe, J. Tyburczy, F. Nestola, Eur. J. Mineral. 21 (2009) 615–622.
[35] T. Yoshino, T. Matsuzaki, A. Shatskiy, T. Katsura, Earth Planet. Sci. Lett. 288 (1) (2009) 291–300.
[36] X. Yang, Earth Planet. Sci. Lett. 317–318 (2012) 241–250.
[37] L. Dai, S. Karato, Earth Planet. Sci. Lett. 287 (2009) 277–283.
[38] L. Dai, S. Karato, Proc. Jpn. Acad. B-Phys. 85 (2009) 466–475.
[39] B. Zhang, T. Yoshino, X. Wu, T. Matsuzaki, S. Shan, T. Katsura, Earth Planet. Sci. Lett. 357 (2012) 11–20.
[40] L. Dai, H. Li, H. Hu, S. Shan, J. Jiang, K. Hui, Contrib. Mineral. Petrol. 163 (2012) 689–700.
[41] T. Katsura, K. Sato, E. Ito, Nature 395 (1998) 493–495.
[42] D. Dobson, J. Brodholt, J. Geophys. Res. 105 (2000) 531–538.
[43] W.L.Du. Frane, J.J. Roberts, D.A. Toffelmier, J.A. Tyburczy, Geophys. Res. Lett. 32 (2005)http://dx.doi.org/10.1029/2005GL023879.
[44] C. Romano, B.T. Poe, N. Kreidie, C.A. McCammon, Am. Mineral. 91 (2006) 1371–1377.
[45] L. Dai, S. Karato, Phys. Earth Planet. Inter. 176 (2009) 83–88.
[46] L. Dai, S. Karato, Earth Planet. Sci. Lett. 408 (2014) 79–86.
[47] L. Dai, S. Karato, Phys. Earth Planet. Inter. 237 (2014) 73–79.
[48] B. Poe, C. Romano, F. Nestola, J.R. Smyth, Phys. Earth Planet. Inter. 181 (2010) 103–111.
[49] K. Ohta, K. Hirose, M. Ichiki, K. Shimizu, N. Sata, Y. Ohishi, Earth Planet. Sci. Lett. 289 (2010) 497–502.
[50] T. Yoshino, A. Shimojuku, S. Shan, X. Guo, D. Yamazaki, E. Ito, Y. Higo, K. Funakoshi, J. Geophys. Res. 17 (2012) B08205, http://dx.doi.org/10.1029/2011JB008774.
[51] R. Sinmyo, G. Pesce, E. Greenberg, C. McCammon, L. Dubrovinsky, Earth Planet. Sci. Lett. 393 (2014) 165–172.
[52] J.A. Tyburczy, D.K. Fisler, in: T.J. Aherns (Ed.), Mineral Physics and Crystallography, vol. 2, AGU, Washington, D. C 1995, pp. 185–208.
[53] J.O. Isard, J. Non-Cryst. Solids 246 (1999) 16–26.
[54] K.A. Foland, in: A.W. Hofmann, B.J. Giletti, H.S. Yoder, R.A. Yund (Eds.), Geochemical Transport and Kinetics, Carnegie Institution of Washington, Washington, D. C 1994, pp. 77–98.
[55] R.B. Kasper, Cation and Oxygen Diffusion in Albite(Ph.D. thesis) Brown University, Providence, Rhode Island, 1975. 143.
[56] T. LaTourrette, G.J. Wasserburg, Earth Planet. Sci. Lett. 158 (1998) 91–108.
[57] H. Behrens, W. Johannes, H. Schmalzried, Phys. Chem. Miner. 17 (1990) 62–78.
[58] D. Cherniak, Rev. Mineral. Geochem. 72 (2010) 691–733.